Project for a
Surface Diffraction Beamline at SOLEIL
(Proposal 17)

ADDENDUM

Contacts: Yves GARREAU (LURE - Orsay)
Victor H. ETGENS (Laboratoire de Minéralogie-Cristallographie – Paris)

With contributions from:

J. DAILLANT (LURE – Orsay)
M. GOLDMANN (LURE – Orsay, OCIIB – Paris)
P. FONTAINE (LURE – Orsay)
C. MALGRANGE (Laboratoire de Minéralogie-Cristallographie – Paris)
A. COATI (LURE – Orsay)
A. BARBIER (DRECAM/SPCSI CEA – Saclay)
T. MORENO (SOLEIL – Saint Aubin)
M. IDIR (SOLEIL – Saint Aubin)

The present document appends the Surface Diffraction Beamline (SDB) proposal 17 and takes into account the recommendations of the SOLEIL Scientific Advisory Committee (June 2002). The SDB beamline has been supported. However, the Scientific Advisory Committee suggested a fusion with part of other SOLEIL projects and also asked for additional information concerning the optics of the beamline. In the meantime, the SOLEIL directorate strongly encouraged a fusion with the high-energy part of the Soft Interfaces Diffraction (SID) beamline project (proposal 20). The scientists involved in both proposals have thus worked together to produce one single, coherent and updated project for a high-energy beamline, which is not detrimental to either of the two initial propositions. However, the mandatory modifications for a beamline set-up fulfilling the needs of both projects result in extra-costs as compared to the initial project. The major modification concerns the multi-purpose diffractometer, which, in addition to the already defined multi-purpose surface diffraction capabilities, must now receive the cumbersome horizontal liquid environment and extra-degrees of freedom to perform reflectivity measurements. Since this aspect was not included in the previous version of proposal 17, a detailed scientific case for buried soft interfaces studies is presented in the following.

Another aspect, which has required our particular attention, is the control of the polarisation of the incoming X-ray beam. In fact one of the highlights of the SDB project concerns the magnetic studies in the energy range between 6 and 9 keV. One should note that when using grazing incidence and thus asymmetric diffraction peaks, the polarisation can no longer be chosen as perfectly parallel or perpendicular to the scattering plane, hence, the classical $\sigma\sigma$, $\pi\pi$, $\pi\sigma$ and $\sigma\pi$ channels are no longer available. In order to obtain the accurate matrix elements (especially when performing resonant diffraction experiments) one has to perform two measurements either by switching the sample surface from vertical to horizontal (which seems mechanically almost impossible to achieve in an UHV surface diffraction set-up) or by switching the linear beam polarisations from horizontal to vertical. Hence, to exploit the full potential of this technique it is mandatory that the beamline offers vertical and horizontal linear beam polarisations together with a strong photon flux. The present beamline layout takes into account this important requirement. The idea is to get a very flexible beamline allowing to switch between horizontal, vertical and circular polarisations in a user friendly way.

The present document is intended to supplement the beamline proposal 17, which was devoted to the properties of solid surfaces studied in ultra-high vacuum, controlled atmosphere and liquid environments (see http://www.synchrotron-

soleil.fr/science/aps/doc/BL17.pdf). We stress that the scientific case reported in the initial document remains fully relevant and is now enriched by the section A of the present addendum. This section contains some aspects developed in proposal 20 (see http://www.synchrotron-soleil.fr/science/aps/doc/BL20.pdf) and opens new perspectives supplied by the X-ray reflectivity measurements, which become available thanks to the multi-purpose diffractometer. In section B we present a detailed description of this diffractometer, adapted to the needs of the soft interfaces studies. Finally, in section C, we describe the beamline optical elements, and we present the ray-tracing and polarisation calculations.

The present document is organized as follows:

A) Buried soft interfaces and systems of biological importance

Soft interfaces are created when at least one of the two media is a liquid, liquid crystal, polymer etc. Since the cohesive energies between molecules in these media are of the order of k_BT, the properties of such interfaces can be strongly modified, for example by intercalating surfactant molecules soluble in only one of the two media. In some cases, these molecules will form a monolayer at the interface, reduce the interfacial tension and more generally modify its properties. Such systems are relevant in many fields of physics, chemistry and biology. In the case of the liquid-air interface, and when the surfactant molecules are insoluble in the liquid phase, they form films called Langmuir films. Moreover, surface interactions at solid-liquid and liquid-liquid interfaces also provide a unique way to orient and manipulate fragile membranes or colloidal particles, which can then be studied in great detail. Finally, they are of fundamental importance in processes of technological relevance like adsorption, corrosion or liquid extraction.

During the last decade, the application of the Grazing Incidence X-ray Diffuse Scattering (GIXDS) and Diffraction (GIXD) to the study of Langmuir films has been responsible for major breakthroughs in this field, giving access to the microscopic structures. However, the application of these techniques to buried interfaces such as liquid-liquid or solid-liquid interfaces has not been so developed. Some experiments on liquid-liquid interfaces have been already successfully performed at high energy both in GIXD and X-ray reflectivity geometry. Such experiments of course take over technical challenges. In most of them a macroscopically thick upper liquid phase is used and the X-ray penetration in the liquid has to be large enough (experimental cells are generally several centimetres wide), which can be achieved using high-energy beams (18-20 keV) [1]. In fact, at the "usual energy" of 8 keV, the transmission through 1 mm of water is 36%, whereas it reaches 93% at 20 keV. Alternatively one can consider thin wetting films [2]; this possibility is however limited to few experimental cases. Another difficulty for the liquid-liquid interfaces is the presence of a meniscus. This problem has been solved either using cells made of different materials and using the bottom liquid level to adjust the interface height [1], or giving the meniscus a saddle shape using a trough with tilted non-parallel edges [3]. The last and most important problem is the scattering background due to the upper phase. Two different strategies have been used to avoid this problem. In Ref. [4], this background is minimized

using microbeams and very small slits for detection. This is very efficient for reflectivity and diffraction, but not for diffuse scattering, where the signal itself scales with the scattering solid angle, leading to a very careful, background subtraction. The second strategy consists in using grazing incidence geometry. In fact, if the incidence angle is below the critical angle for total external reflection [1], signal as small as 1% of the bulk scattering in the upper phase can be measured in a reliable way as demonstrated by measurements on model systems and detailed calculations.

Unfortunately, only one instrument located at the CRG-IF beamline using a bending magnet source of the ESRF in Grenoble, is available providing both high-energy X-rays and an environment adapted to soft/liquid interfaces. Two instruments (GMT and SUV) share this beamline, leading to a very limited beamtime. In this context, an optimised goniometer for soft interfaces together with an undulator source providing in-plane parallel beam (weak in-plane divergence) and high flux at high energy (20 keV) would open a new opportunity for the user's community.

In the following, we give some examples of highlight research fields, which could benefit of such beamline. Some of these topics have been better detailed in the SID beamline proposal (http://www.synchrotron-soleil.fr/science/aps/doc/BL20.pdf).

Buried soft interfaces

Liquid-liquid interfaces present a great interest due to the numerous problems in which they are involved. For example, understanding the adsorption properties of various compounds, as amphiphile molecules at the oil-water interface, is of main importance for pollution problems. Applications are expected as well in water purifications (by using cage molecules for trapping impurities and adsorbing them on the surface covered by an oil film) or for dispersing oil in water. Fundamental studies of liquid-liquid interfaces have been mainly undertaken in Mark Schlossman's group in Chicago using X-ray reflectivity. They could show that the width of the alkane-water interfaces results from the convolution of an intrinsic width with capillary wave fluctuations. They proposed that the intrinsic width is determined by the radius of gyration for the shorter alkanes and by the bulk correlation length for the longer alkanes [2]. Of course, this is only one example and much remains to be done, in particular using diffuse scattering to probe the effects of different interactions and mechanisms at various length-scales as recently achieved for liquid-vapour interfaces [5,6].

The properties of liquid-liquid interfaces can be dramatically modified in presence of amphiphilic molecules. The interfacial tension can for example be decreased by several orders of magnitude in microemulsion phases. A few scattering experiments have addressed on these systems [7,8]. The feasibility of such experiments has been demonstrated, but, up to now, no significant results have been obtained. A comprehensive understanding of the relationship between interfacial tension and the molecular organization across the interface remains a challenging goal. Beyond interfacial tension, bending rigidity is another important parameter determining the structure and properties of complex fluids. Preliminary determinations could be obtained for phospholipid monolayers [1] and charged diblock copolymers [9]. Again, the relationship between molecular organization and bending rigidity as well as the very nature of this quantity [5] are still open questions.

In addition to scattering techniques, the possibility of performing grazing incidence fluorescence experiments will provide a very powerful tool combining the depth sensitivity of the evanescent wave with the chemical sensitivity of fluorescence in order to precisely locate atoms across a complex interface. This has, up to date, only been performed at the liquid-vapour interface but could be extended to liquid-liquid interfaces when using a thin wetting film as upper phase.

Self-assembled films are obtained by merging a solid substrate in a solution of self-assembled molecules. These films have a great application potential, ranging from microelectronics to biotechnologies. Understanding the film formation mechanism is a key step in controlling the final properties of the surface. Although the final structure of such films has been observed by different techniques including GIXD at the solid–air interface, the kinetics of formation of these films is difficult to investigate since the incident X-ray beam has to penetrate through the solution. An instrument providing high energy X-ray will enable the study of this process at a molecular level. Both the lateral arrangement of the molecules (GIXD) and the vertical structure of the layer (X-ray reflectivity) can be investigated.

Another interesting field is the study of the interface formed by a liquid crystal films and a polymer or a solid substrate (single crystal or not). Indeed, the applications of such systems, especially in opto-electronics, are closely related to the anchoring properties of the liquid crystal, which often impose the properties of the liquid crystals bulk phase. When the liquid crystal film is thick, the problem of the absorption of the incident and scattered beam can be overcome by the use of high energy X-rays.

It should also be noticed that beyond the experiments in electrochemistry presented in the original proposal 17, the beamline would greatly benefit from the combined experience of

surface diffraction and liquid environment. By this way one can perform the study of the structure of a solid surface and its modifications due to the presence of a liquid. A first example is the interaction of liquid water with surfaces of natural solid oxides like aluminosilicate clays, which has been performed at the APS [10]. In the same spirit, characterizing structures like surface micelles in adsorption processes or performing detailed studies of corrosion will be possible.

Some fundamental features of solid-liquid interfaces have been evidenced using scattering techniques, in particular by Helmut Dosch's group in Stuttgart. They observed few well-defined molecular layers at the liquid metal free surface [11]. This layering results surprisingly deep in the case of a liquid metal/solid interface, respect to what is evidenced in the case of a liquid metal free surface [12]. Another important experimental result is the observation of five-fold symmetry of icosahedral clusters at the (liquid lead)-solid interface. These clusters were assumed to be present in the liquid, but their observation was only possible thanks to the ordering imposed by this interface, which reduces the rotational averaging [13].

Standing wave experiments can help in obtaining detailed information [14,15]. They have been used for example to study membranes and a diffuse ionic double layer. The chain-end distribution in a polyisoprene brush with end-grafted Ge atoms has been recently determined using this technique [16].

As mentioned in the introduction, interfaces can also be used to orientate membranes and investigate their properties in greater detail. This has been done for phospholipid membranes close to a solid wall [17]. It is indeed possible to trap a lipid membrane on a silicon substrate coated with a grafted silane monolayer and a first lipid monolayer exposing its heads toward water. Surprisingly, the fluctuations of this single membrane in water can be characterized in detail using diffuse scattering, and its residual tension, bending rigidity and interactions with the wall can be determined very precisely, opening wide possibilities.

Systems of biological relevance

Langmuir monolayers (at the air-water interface) have been widely used to study interactions between membranes and biological molecules. In these studies, a phospholipidic monolayer is used to mimic the membrane as the biological molecules are introduced into the liquid subphase. The observation of the film structure modification allows determining how strong, oriented or specific the interaction is. However, in real cell, the membrane is a bilayer

formed by head to tail phospholipids and such structure is unstable at the air-water interface. The study of buried interfaces, where such bilayer can be stabilized and then of more biological relevance, may be important to confirm the obtained results. In addition, other buried interfaces can be considered. A phospholipidic monolayer deposited at the water–alkane interface may describe the behaviour of half a membrane. In this situation, the hydrophobic part of the phospholipid molecules is in contact with the alkane phase. The interactions are then more realistic between the monolayer and the upper medium compared to the air-water interface. Another buried interface of biological relevance is the solid – liquid interface with a bilayer deposited onto the solid substrate. In such a configuration, the influence of the wall on the membrane fluctuations can be studied. For "passive" membranes, it is now well established that the presence of a wall (or another membrane) gives rise to a long-range interaction of entropic origin, the "Helfrich" interaction. However, if active proteins (*i.e.* ion channel) are incorporated in the bilayer, it becomes active and the fluctuation spectrum is strongly modified. Attempt has been made to observe this modification by using Reflection Interference Contrast Microscopy (RICM) on giant vesicles. The previous system offers an attractive alternative to evidence such effect. This last project will require not only the use of neutrons and X-ray reflectivity but also of diffuse scattering in order to access to much shorter length scales of fluctuations than optical microscopy.

Langmuir monolayers have also been used to promote 2D protein crystallisation. In this case, one incorporates specific ligand of the studied protein in the monolayer. The proteins are fixed under the surface by the ligand and one expects that they will crystallise when a surface density threshold is reached. Such procedure presents the advantage to need few protein material (2D crystal) and, if the ligand is really specific, a weaker purification of the biological material. Once the 2D crystal is formed, it can be transferred or directly observed by surface diffraction. However, in this last case, one needs high-energy X-rays (minimum 13 keV) to reduce the sample degradation. Moreover, high-energy photons are definitively needed to study membrane protein 2D crystal. Indeed, when the proteins are not soluble in water, the previous process is non-operant. A proposed solution is then to include the proteins into micelles formed by detergent added in the solution. However, this new subphase (water + detergent) wet the Teflon and then the edges of the through. To avoid an overflow, one uses a modified Langmuir trough, which is not completely filled. To perform X-ray scattering measurement, Kapton or Teflon windows are made in the through edges. However, the liquid meniscus climbs on these windows and thus, the X-ray beams (incident and scattered) have to cross these meniscuses. Such experiments have been successfully

attempted on Langmuir monolayers deposited at detergent solution – air interface by using the "GMT goniometer" of the ESRF-CRG IF and 18 keV photons energy [18].

References:

[1] C. Fradin, D. Luzet, A. Braslau, M. Alba, F. Muller, J. Daillant, J.-M. Petit, and F. Rieutord « X-ray study of the fluctuations and of the interfacial structure of a phopholipid monolayer at the alkane-water interface », Langmuir **14**, 7327 (1998).
[2] M. Li, A. M. Thikonov, D. Chaiko and M. L. Schlossman, « Coupled capillary wave fluctuations in thin aqueous films on an aqueous subphase », Phys. Rev. Lett. **86**, 5934 (2001); S. Mora, J. Daillant, M. Alba, D. Luzet, unpublished.
[3] D. M. Mitrinovic, A. M. Thikonov, M. Li, Z. Huang and M. L. Schlossman, « Non capillary-wave structure at the water-alkane interface », Phys. Rev. Lett. **85**, 582 (2000).
[4] H. Reichert, V. Honkimäki, A. Snigirev, S. Engemmann and H. Dosch, « A new X-ray transmission-reflection scheme for the study of deeply buried interfaces using high energy microbeams » Physica B **336**, 46 (2003).
[5] C. Fradin, A. Braslau, D. Luzet, D. Smilgies, M. Alba, N. Boudet, K. Mecke and J. Daillant, « Reduction in the surface energy of liquid interfaces at short length-scales » Nature **403**, 871 (2000).
[6] S. Mora, J. Daillant, K. Mecke, D. Luzet, A. Braslau, M. Alba and B. Struth, « X-ray synchrotron study of liquid-vapor interfaces at short length-scales: effect of long-range forces and bending energies » Phys. Rev. Lett. **90**, 216101 (2003).
[7] B. R. McClain, D. D. Lee, B. L. Carvalho, S. G. J. Mochrie, S. H. Chen and J. D. Lister, « X-ray reflectivity study of an oil-water interface in equilibrium with a middle phase microemulsion », Phys. Rev. Lett. **72**, 246 (1994).
[8] D. M. Mitrinovic, S. M. Williams and M. L. Schlossman, « X-ray study of oil-microemeulsion and oil-water interfaces in ternary amphiphilic systems », Phys. Rev. E **63**, 021601 (2001).
[9] G. Romet-Lemonne, thesis, Paris-sud (2002).
[10] P. J. Eng, private communication.
[11] C. J. Yu, A. G. Richter, J. Kmetko, S. W. Dugan, A. Datta and P. Dutta, « Structure of interfacial liquids: X-ray scattering studies », Phys. Rev. E **63**, 021205 (2001); H. Kim, O. Seeck, D. R. Lee, I. D. Kandler, D. Shu, J. K. Basu and S. K. Sinha, « Synchrotron X-ray studies of molecular ordering in confined fluids », Research society symposium proceeding, vol. 651 (2001).
[12] H. Dosch, H. Reichert, private communication
[13] H. Reichert, O. Klein, H. Dosch, M. Denk, V. Honkimäki, T. Lipmann and G. Reiter, « Observation of five-fold local symmetry in liquid lead », Nature **408**, 839 (2000).
[14] M. J. Bedzyk, G. M. Bommarito, M. Caffrey, T. L. Perner, « Diffuse double layer at a membrane aqueous interface measured with X-ray standing waves », Science **248**, 4951 (1990); R. Zhang, R. Ihi, M. Caffrey, « Membrane structure characterization using variable period X-ray standing waves », Biophys. J. **74**, 1924 (1998).
[15] J. Basu, J. C. Boulliart, J. Daillant, P. Guenoun, unpublished.
[16] J. C. Boulliard, private communication.
[17] G. Fragneto, F. Graner, T. Charitat, E. Bellet-Amalric, A. Braslau, J. Daillant, unpublished.
[18] P. Fontaine, F. Muller, M. Poujade, M. C. Fauré, M. Goldmann, J. S. Micha, F. Rieutord, D. Levy, submitted to Langmuir (Sept 2003).

B) Description of the "multi-purpose" diffractometer

In the original Surface Diffraction Beamline APS we have proposed a "multi-purpose" diffractometer, dedicated to the non-UHV studies (*i.e.* electrochemical environments, special sample environment). The association with the Soft Interfaces Diffraction project implies improvements of this device in order to satisfy the special configuration required for liquid diffraction and reflectivity measurements. The main requirements that must be fulfilled by the instrument are the followings:

- The diffractometer needs a vertical axis together with an important vertical translation able to hold heavy (20 kg) and large samples with their environments, for instance a goniometer head supporting a Langmuir trough with its active anti-vibration table.
- To perform specular X-ray reflectivity measurements on liquid surfaces, due to intrinsic horizontal nature of the liquid interfaces, the beam has to be deflected downward. To measure the specular reflectivity with a convenient transfer wave vector range, one needs to access angles larger than those reachable by mirrors, even coated with heavy elements. A single crystal (silicon, germanium) in Bragg or Laüe geometry can be used to deflect the beam, requiring then a small goniometer to align the crystal (it will be also used to adjust a deflecting-mirror for grazing incidence liquid surface diffraction experiments). However, in this geometry, deflecting vertically the incident beam (by rotating the deflecting-crystal) induces also a deflection along the horizontal direction. Consequently, the sample diffractometer should be able to rotate on a horizontal circle centred on the deflecting-crystal. Of course, a vertical translation of the diffractometer is also needed to take into account the variation of the incidence angle. Such experimental set-up is already operating on other facilities, like APS or Brookhaven (www.solids.bnl.gov/lss/; http://www.solids.bnl.gov/home/ben/liquids.html).
- In order to have access to the whole reciprocal space, the detector arm needs two degrees of freedom (two circles) and has to support heavy detection equipment (analyser + detector).
- The overall resolution of both the sample diffractometer and the deflecting crystal goniometer should be good enough to enable the study of single crystals (*i.e.* 0.0001° resolution for the sample circles).

As an example, a commercial solution, which satisfies the experimental requirements already mentioned, is depicted in Fig.1. It comes from the Newport-Microcontrole Inc. division for large diffractometer. The sample diffractometer consists in a base table bearing a horizontal circle with a vertically mounted circle supporting the detector arm (*i.e.* a classical X95), which can host a large detection system. On such table, the sample is supported by a "tower" providing all the degrees of freedom for sample positioning. For scattering on liquid systems, this tower allows the required vertical translation to align the liquid surface with the beam, an XY stage for the sample translation and two goniometric cradles to align the through containing the liquid with the horizontal direction.

The resolution of the detector circles is 0.00025° for the horizontal one and 0.001° for the vertical one. The detector arm can bear a maximum load of 45 kg at 500 mm from the goniometer's centre. The goniometer base moves vertically of 175 mm and horizontally of 100 mm (along the direction normal to the beam). The sample tower can bear sample chambers of about 30 kg with 0.1 µm resolution on the vertical stage and a range of 100 mm. The XY stage can move the sample of ± 25 mm. The "tower" allows a rotation of the sample with a resolution of 0.0001° and the cradle has a resolution of 0.0001°. The sample diffractometer (base + tower) has to move on a horizontal circle centred on the deflecting crystal; to this aim it is mounted on a horizontal arm moving on a circle centred at 1 m from the centre of the sample diffractometer. Centred with this circle, a "tower" bears a smaller goniometer on which the deflecting crystal needed for the liquid surface reflectivity is mounted. The "deflecting crystal" tower has the same characteristics than the liquid sample tower.

This solution is very flexible, allowing using the same diffractometer for other applications by simply changing the sample "tower" (with a good reproducibility of the sphere of confusion). In this way different experiments, requiring different sample environments, can be performed on the same instrument. There exists also an option to mount the sample vertically for specific experiments concerning solid surfaces. For example, we show in Fig.2 the diffractometer (based on the standard Newport-Microcontrole Inc. X95 model), located at the ESRF BM26 beamline, which permits different configurations (*e.g.* diffraction with a horizontal or vertical surface) with various sample environments.

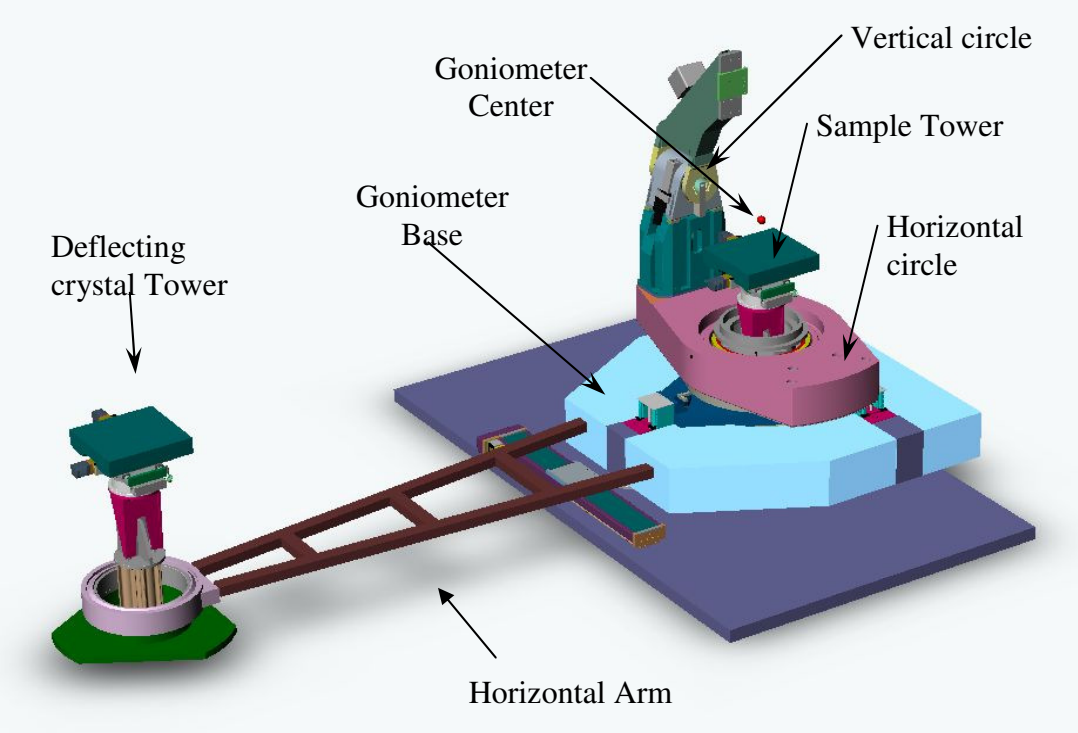

Figure 1: Schematic representation of the "multi-purpose" diffractometer (Newport-Microcontrole Inc.). The element scales are not respected in the figure.

Figure 2: Diffractometer design by E. Newport-Microcontrole Inc. (X95 basis) at ESRF BM26 beamline.

C) The optics of the beamline with ray-tracing and polarisation calculations

We have studied and revised the beamline optics especially considering the beam polarisation requirements. Ray-tracing calculations were performed taking into account different configurations and solutions, in order to obtain the best compromise between the following beam characteristics: (*i*) flux (focalisation), (*ii*) spectral resolution (monochromator) and (*iii*) beam divergence, which are crucial for obtaining a good polarisation rate by means of phase plate devices.

In the following we describe the optimised configuration of the optical elements of the beamline and their functions. Finally, we present the ray-tracing simulations and the polarisation calculations.

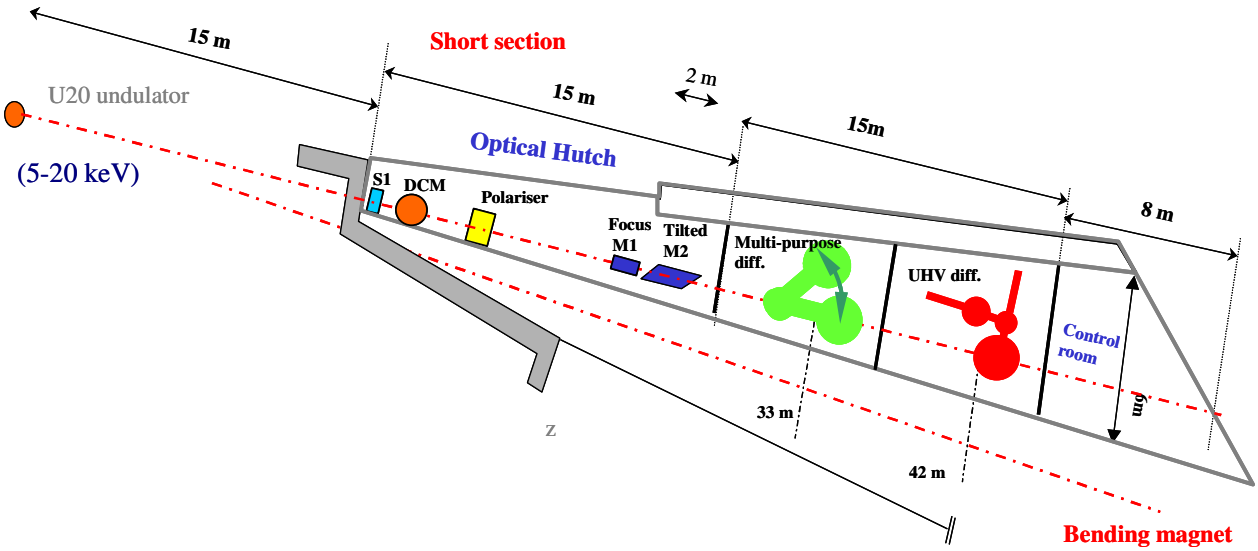

Figure 3: Schematic layout of the beamline optical elements. The individual positions with respect to the source are reported in Table 1.

Component	Distance from the source	Dimensions
Slit (S1)	15 m	2 x 0.7 mm^2
Monochromator (DCM)	16.5 m	40 x 40 x 10 mm^3
Phase Plate Device	20 m	-
Mirror 1 (M1) (vertical focusing)	26 m	20 x 350 x 20 mm^3
Tilted mirror (M2) at 45°	28 m	20 x 550 x 20 mm^3
"Multi-purpose" Diffractometer	33 m	-
UHV-Diffractometer	42 m	-

Table 1: Positions of the beamline optical elements with respect to the beam source.

Source

The X-rays source is an U20 undulator placed on a short section. The electron source parameters are listed in the following table. σ_x and σ_z are the beam dimensions along the horizontal (x) and the vertical (z) directions respectively, while $\sigma'_{x,z}$ are the beam divergences. We stress that the beam shape is strongly anisotropic.

	σ_x (µm)	σ_z (µm)	σ'_x (µrad)	σ'_z (µrad)
Short Section (L=1.8 m)	**388**	**8.1**	**14.5**	**4.61**

Primary slits (S1)

The primary slits are fixed at 2 x 0.7 mm^2, calculated in order to absorb efficiently the thermal power (about 3.7 kW) and to transmit 95% of the 3rd harmonic at 5 keV.

Double Crystal Monochromator (DCM)

The energy will be selected by a double-crystal monochromator, located at 16.5 m from the source point, with fixed-exit. In this configuration, with about 150 W of thermal power, it is mandatory to have a cryogenically cooled first crystal. The optical system is designed to be tunable from 4 to 20 keV using Si(111) crystals, with an angular accessible range varying from 5 to 30°.

First Mirror (M1)

The first mirror M1 is located at 26 m from the source point. This silicon crystal mirror, partially coated with a 50 nm layer of Pd, will be elliptically bendable allowing the beam to be focused on the sample.

The beam incident angle on M1 will be kept fixed and equal to 0.175° (3 mrad). The uncoated part of the Si mirror is well suited for the 4-10 keV energy range, whereas the metal-coated stripe is more appropriate for high energies, between 10 to 20 keV. This mirror acts also as a low-pass filter and will reject high-energy beams due to high order harmonics.

Second Mirror (M2)

The second mirror accomplishes two main functions, closely connected to the experimental geometry (*i.e.* working with a vertical or a horizontal surface):

a) When using vertical surfaces (*e. g.* UHV diffractometer), M2 is tilted at 45° with respect to the horizontal plane. At this particular position, it produces the exchange of the source size/divergence between the vertical and horizontal directions. This produces a beam shape well adapted to grazing incidence geometry. The ray-tracing results presented in the following tables are calculated in this configuration.
b) When using a horizontal surface (*e.g.* liquid diffraction), M2 is not tilted, allowing obtaining a horizontal beam and also acting as a second mirror for harmonics rejection.

The same incidence angle and the same coating as for the first mirror M1 will be used.

Polariser

The adjustable polarisation will be obtained through phase plate devices according to the needs for circular or vertical linear polarisation. The polariser effects are not taken into account in the ray-tracing calculations. The performances of the phase plate device are presented in the last section.

Ray-tracing simulations

In the following table we present the results of the ray-tracing simulations. The calculations were performed considering the configuration discussed above. Reasonable mirror roughness (σ = 3 Å RMS) and longitudinal slope errors (ε = 0.3" RMS (1.5 µrad RMS)) were also taken into account. The flux (N), the energy dispersion (ΔE), the FWHM beam dimensions ($\Sigma_{x,z}$) and divergences ($\Sigma'_{x,z}$) on the sample were calculated for four different energies (5, 10, 15 and 20 keV). The calculations were performed considering a focused beam (with M1 elliptically bended). The sample was considered fixed at 33 m or at 42 m from the source point that corresponds to the location of the "multi-purpose" and the UHV diffractometers respectively. In the following table we report also the beam characteristics calculated at the phase plate position.

Position	E (keV)	N (ph/s)	ΔE (eV)	Σ_x (μm)	Σ_z (μm)	Σ'_x (μrad)	Σ'_z (μrad)
Phase Plate Device (20 m)	5	1.27×10^{14}	0.65	1174	568	39.3	28.3
	10	3.55×10^{13}	1.54	1164	501	37.5	25.4
	15	1.38×10^{13}	2.45	1139	330	34.9	16.6
	20	3.04×10^{12}	4.97	1144	477	35.9	23.8
"Multi-purpose" Diffractometer (33 m)	5	1.02×10^{14}	0.65	51.4	1538	100	37.0
	10	2.93×10^{13}	1.55	51.8	1507	89	36.6
	15	1.11×10^{13}	2.39	49.5	1435	58.0	35.5
	20	2.10×10^{12}	4.66	50.1	1438	62.0	34.9
UHV Diffractometer 42 m	5	1.02×10^{14}	0.65	123.7	1729	39.2	37.4
	10	2.93×10^{13}	1.54	122	1786	38.4	36.3
	15	1.11×10^{13}	2.40	123	1760	33.3	35.5
	20	2.10×10^{12}	4.66	121	1700	33.4	35.3

Table 2: Results of the ray-tracing simulations.

Considering the ray-tracing results, we note that the mirror M_2 acts as a "XY beam inverter" in a very satisfactory manner. We can observe that the beam dimensions on the sample in the focused mode at 33 m are (50 x 1500) μm², and at 42 m is (125 x 1800) μm². For the case of the liquid diffraction, if we consider a simple M2 mirror (not tilted), the beam dimensions are also satisfactory.

Polariser

An adjustable polarisation can be obtained by means of a phase plate device using the forward-diffracted beam by a diamond crystal [1]. A good quality diamond crystal adjusted close to Bragg diffraction, here (111) reflection, introduces a phase-shift between the two components, respectively polarised in the plane of diffraction (π component) and normal to this plane (σ component) of the forward-reflected beam. The phase-shift φ is inversely proportional to the departure from Bragg angle of the incident beam or "offset" $\Theta = \theta - \theta_B$ (where θ is the angle of incidence on the diffracting planes and θ_B the Bragg angle) and "naturally" proportional to the beam path *t* of the beam in the crystal.

$$\varphi = A\frac{t}{\Theta}$$

If the plane of diffraction of the diamond plate makes a 45° angle with the horizontal plane, the incident polarisation, which is horizontal, has two equal σ and π components. If the phase-shift introduced by the phase plate is equal to +90° (respectively –90°) the transmitted beam is right (respectively left)-circularly polarised. If the phase-shift is equal to 180° the transmitted

beam is vertically linearly polarised. The variation of the phase-shift is easily obtained by a variation of the offset, *i.e.* a rotation of the diamond crystal around the normal to the plane of diffraction. The same device makes then possible to obtain vertically polarised and circularly polarised photons and also to switch from right to left circularly polarised photons by a simple rotation of the diamond crystal.

The rate of polarisation is not strictly equal to 1 because the beam has non-zero angular and spectral divergences introducing a dispersion $\Delta\Theta$ of the offset Θ through the dispersion on the angle of incidence θ and on the Bragg angle θ_B respectively. The offset to get circular polarisation being two times larger than the one to get linear vertical polarisation, the integration on $\Delta\Theta$ has less influence on circular polarisation rate than in the case of linear polarisation rate (Fig. 4).

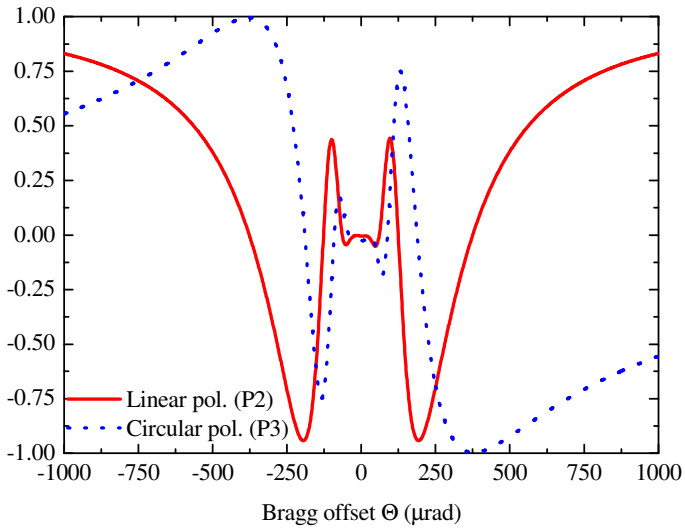

Figure 4. Variation of the linear polarisation rate P_2 (red line) and the circular polarisation rate P_3 (blue dot line) as a function of the offset Θ for a diamond phase plate (beam path of 2 mm) for 9 keV photons and a 50 µrad FWHM gaussian divergence. A circular polarisation rate of 1 (exactly $P_3 = 0.996$) is easily obtained for an offset around 380 µrad whereas the maximum vertical linear polarisation rate is 0.94 ($P_2 = -0.94$), obtained for an offset of 195 µrad.

Furthermore X-ray Magnetic Circular Dichroism (XMCD) signals are proportional to the rate of polarisation so that a small decrease of this rate only decreases a little the amplitude of the XMCD signal. On the contrary, magnetic diffraction experiments require a high rate of linear polarisation. It is clear that the influence of a given dispersion of the offset

is the smaller the larger the "exact" offset is. A larger “exact” offset is obtained by increasing the beam path in the diamond plate but this induces a larger absorption.

Fig. 5 shows the variation of the vertical linear polarisation rate as a function of the offset for three different beam-paths and the same angular dispersion of 50 µrad.

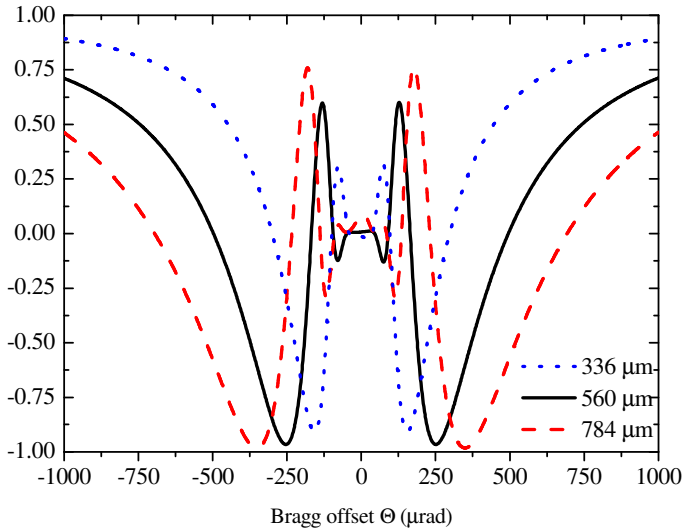

Figure 5: Linear polarisation rate P_2 as a function of the offset for 6 keV photons for three different beam-paths: 336 µm (blue-dot curve), 560 µm (black) and 784 µm (red-dash), leading to respecting transmission coefficients equal to 0.31, 0.14 and 0.063. A vertical linear polarisation is obtained for $P_2 = -1$.

It is clear that the linear polarisation rate increases with the beam-path because the working value of the offset increases but then the absorption increases. One has to find a good compromise between the polarisation rate and the transmission of the phase plate. In order to give numbers for the influence of the offset dispersion $\Delta\Theta$ on the polarisation rate, Fig.6 present curves for the linear vertical polarisation rate as a function of the transmission for different values of the offset dispersion $\Delta\Theta$, for two extreme X-ray energies 6 keV and 9 keV (Fig.6). Taking into account the angular and spectral divergence of the beam (see Tab.2) one expects to get a resulting dispersion of the offset $\Delta\Theta^{(*)}$ equal to 82 µrad at 6 keV and 58 µrad at 9 keV. A rate of linear vertical polarisation of 90% is obtained with a transmission equal or larger than 15% whereas a polarisation rate of 95% is obtained with a transmission of the order of 7%. In order to cover the energy range from 6 to 9 keV at least two different (111)

diamond crystals with different thickness (about 0.7 and 1 mm) are necessary. It would not be more interesting to use a (311) silicon monochromator because for a given polarisation rate the gain due to the much smaller dispersion of the spectral offset is counterbalanced by the loss of intensity reflected by the monochromator.

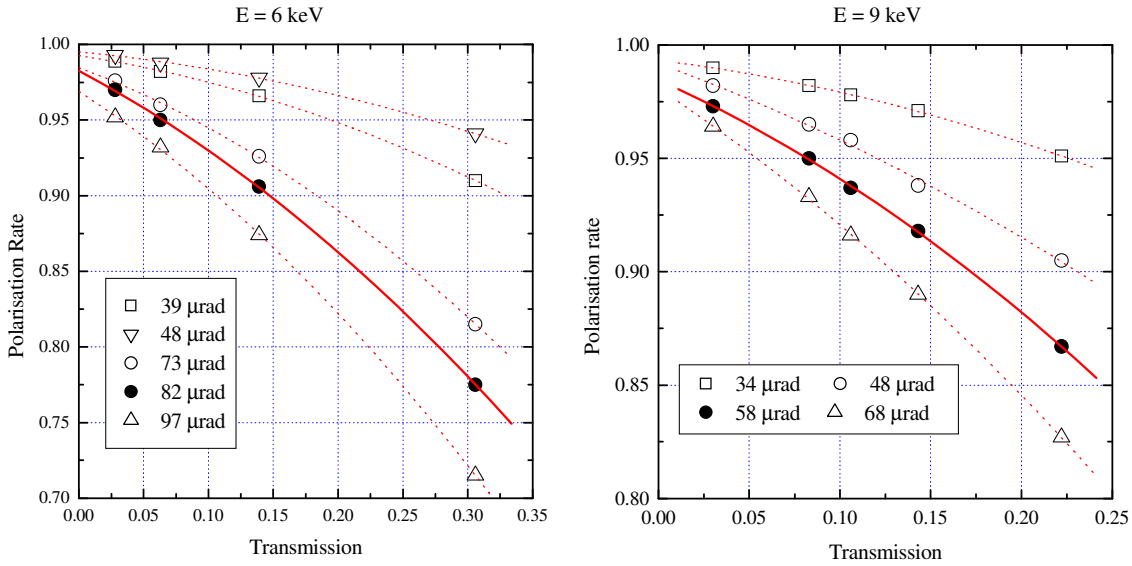

Figure 6: Vertical linear polarisation rate as a function of the transmission for the energies 6 keV and 9 keV. The bold curves correspond to the divergence expected on the beamline.

If the combined rate of polarisation and transmission would happen to be not fully satisfactory one could increase significantly the polarisation rate without loss of intensity by using two successive phase plates with the same total thickness. The set-up would consist of two diamond phase plates rotated 90° around the incident beam one with respect to the other [2, 3]. This would compensate to the first order the spectral and horizontal divergences. To explain briefly the principle, imagine the second plate is rotated 180° around the incident beam with respect to the first one. Then an incident beam with an incident angle $\Theta + \Delta\Theta$ on the first crystal would have an incident angle $\Theta - \Delta\Theta$ on the second one which cancel, to the first order, the variation of phase-shift due to the divergence in the plane of diffraction here inclined 45° with respect to the vertical plane. This is the reason why some place has to be left along the beam line to put a second goniometer for a second phase plate if necessary.

(*) $\Delta\Theta = \sqrt{(\Delta\theta)^2 + (\Delta\theta_B)^2}$, with $\Delta\theta_B = \left(\Delta E / E\right)\tan(\theta_B)$ and $\Delta\theta = \sqrt{2}/2\left(\Sigma'_x + \Sigma'_z\right)$, where ΔE, Σ'_x and Σ'_z are extrapolated from Tab.2.

[1] C. Giles, C. Malgrange, J. Goulon, F. de Bergevin, C. Vettier, E. Dartyge, A. Fontaine, C. Giorgetti, S. Pizzini; J.Appl.Cryst. (1994), 27, 232-240.

[2] F.de Bergevin, Private communication.

[3] Kokitsu, Y.Ueji, K.Sato and Y.Amemiya; Acta Cryst.A, (2002), 146-154.